Rivadeneyra et al., Expert Opin Environ Biol 2016, 4:2
http://dx.doi.org/10.4172/2325-9655.1000130

Expert Opinion on Environmental Biology

Research Article A SCITECHNOL JOURNAL

# The influence of Salt Concentration on the Precipitation of Magnesium Calcite and Calcium Dolomite by *Halomonas Anticariensis*

**Almudena Rivadeneyra[1*], María Angustias Rivadeneyra[2], Cristóbal Verdugo Escamilla[3],Agustín Martín Algarra[4], Antonio Sánchez Navas[5], and José Daniel Martín-Ramos[5]**

[1]*Department of Electronics and Computer Science, School of Informatics and Tele communications Engineering, University of Granada, Spain*

[2] *Department of Microbiology, Faculty of Pharmacy, University of Granada, Spain*

[3]*LEC-IACT, Avdade Las Palmeras nº 4, 18100, Armilla (CSIC-UGR) Granada, Spain*

[4]*Department of Stratigraphy and Paleontology, Faculty of Science, University of Granada, Spain*

[5]*Department of Mineralogy and Petrology, Faculty of Science, University of Granada, Spain*

[*]**Corresponding author:** Almudena Rivadeneyra, Department of Electronics and Computer Science, School of Informatics and Tele communications Engineering, University of Granada, 18071-Granada, Spain, Tel: +34-958243874; E-mail: arivadeneyra@ugr.es

**Rec date**: Dec 18, 2015 **Acc date**: Feb 15, 2016 **Pub date:** Feb 19, 2016

## Abstract

This research focuses on the formation of Ca-Mg carbonates by *Halomonas anticariensis* in solid media at different salt concentration and incubation time, and discusses the possible role of metabolic activity, bacteria surfaces and carbonic anhydrase in precipitation. Mineral saturation indexes of the solutions indicate that inorganic precipitation of different carbonates is possible in all media used but their precipitation did not occur in sterile control experiments. On the other hand *H. anticariensis* produced different Ca-Mg carbonates depending on salt concentration and $Mg^{+2}/Ca^{+2}$ ratios, in spite of its weak carbonic anhydrase activity. Incubation time does not influence the nature of the precipitates. At low salinity *H. anticariensis* precipitates magnesium calcite. A Ca-Mg carbonate phase with very small particle size, high lattice distortion (strain) and lattice parameters similar to those of disordered kutnohorite is presented and this phase is here referred to as non-stoichiometric calcium- rich dolomite, formed at high salinity. These Calcium-rich dolomites are rarely present in most natural habitats because this phase is thermo dynamically 32 metastable and it is subsequently transformed into calcite and dolomite.

**Keywords:**
Mg-calcite; Calcium-rich dolomite; Protodolomite; Kutnohorite; *Halomonas anticariensis*; Carbonic anhydrase

## Introduction

The implication of microorganisms in mineral precipitation is commonly acknowledged for a wide variety of minerals [1]. Bio mineralization provides valuable insights into geological processes that occurred in recent and ancient times, helps to explain the origin and evolution of life on Earth and can provide data on extra-terrestrial life [2,3].

Microbial involvement in carbonate precipitation has been amply observed and studied both in natural environments and laboratory experiments [4-12]. Mechanisms proposed for bacterially mediated precipitation of carbonate minerals include metabolic activities and/or mineral nucleation, though there is some controversy as to whether their role is active or passive [13-16].

Halophilic bacteria thrive in a wide variety of saline and hyper saline natural environments, where carbonate precipitation frequently occurs. Previous research highlights that these bacteria can precipitate carbonates and other minerals [6,7,17,18]. Such studies provide a deeper understanding of the role of halophilic bacteria in the precipitation of minerals in laboratory cultures and in natural habitats. In particular, since these bacteria abound in a wide range of saline concentrations, they can be used to determine how the ionic composition of the environment affects carbonate precipitation.

According to previous studies, *Halomonas anticariensis*, a moderately halophilic bacterium, precipitates different carbonate minerals, among them a Ca-Mg kutnohorite-type carbonate [19]. Kutnohorite, $CaMn(CO_3)_2$, is a member of the dolomite group [20] and very little is known about its precipitation in natural environments and laboratory cultures. A more in-depth knowledge of the precipitation of Mg-Cakutnohorite-type carbonate would presumably lead to a better understanding of the formation of dolomite, a mineral whose origin and precipitation in recent and ancient environments is controversial (the so-called dolomite problem [21,22]).

In this contribution, we have studied the ability of *H. anticariensis* to form carbonate minerals at different marine salt concentrations and incubation times, and the extent of the precipitation, mineralogy and morphology of the carbonate bioliths formed. We have also dealed with the relation between carbonate precipitation and carbonic anhydrase activity. We have proposed the term calcium dolomite for calcium and magnesium carbonates with a kutnohorite-type structure and with $Ca^{+2}/Mg^{+2}$ ratio values greater than 1 and, finally, we have discussed the mechanisms involved in its bacterial precipitation.

## Materials and Methods

### Microorganisms

The moderately halophilic bacterium *H. anticariensis* was isolated from soil samples collected from the temporarily emerged banks of the Laguna Redonda, in the Fuente de Piedrasaline-wetland wildfowl reserve, Antequera, Spain [23]. The study was made with *H. anticariensis* FP35T (LMG 22089T=CECT 5854T) type strains [24], which are straight, Gram-negative rods, encapsulated and motile. This bacterium is chemo-organotrophic and aerobic.

### Culture media

A modified culture halophilic medium with the following composition (w/v) was used: 1% yeast extract; 0.5% proteose-peptone; 0.1% glucose; 0.4% calcium acetate, 2% bacto-agar, supplemented with a balanced mixture of sea salts (Subow 1931) to final concentrations of 2.5%,7.5%, 15%, and 20% (w/v). The pH was adjusted to 7.2 with 1 M

KOH. The quantities of carbon, nitrogen, and phosphorus from the decomposition of the organic nutrients 77 in all media are the following: C=7.930 $gL^{-1}$; P=0.150 $gL^{-1}$; N=1.728 $gL^{-1}$.

## Crystal formation

*H. anticariensis* was surface-inoculated onto solid media at salt concentration of 2.5%, 7.5%, 15%, and 20%, and incubated at 32°C. The plates were periodically examined by optical microscopy to detect the presence of crystals. These experiments were carried out in triplicate. In all of the experiments, un inoculated culture media and media inoculated with autoclaved bacterial cells were used as a control. After incubation periods of 30 and 75 days, the minerals formed at different salt concentrations were collected and purified for mineralogical and textural study. The precipitates were removed from the medium by placing the agar blocks in water and heating them until ebullition point, allowing the dissolution of the agar. The supernatants were decanted, and the sediments re suspended and washed in distilled water. When the precipitates were free of impurities, they were air-dried at 37°C.

The pH evolution was measured with a pH Meter Basic 20 (Crison).

## X-ray diffraction (XRD) study

All precipitates were examined by powder XRD using a Philips PW 1710/00 diffractometer with a graphite monochromator, automatic slit, Cu Kα radiation, and an on-line connection with a microcomputer. Data were collected during a 0.4 s integration time in 0.02°2θ steps at 40 kV and 40 mA in a 2θ interval of 3-80°. Data processing was performed using the X Powder 12 program in order to obtain qualitative, quantitative, and micro textural mineral analysis [25,26]. X Powder uses nonlinear minimum square procedures to calculate unit-cell axis and their standard deviations. Mean values of $Mg^{+2}/Ca^{+2}$ atomic ratio expressed as x/(1-x) were obtained for Ca-Mg rhombohedra carbonates from the unit-cell parameters. Calculation involved refinement of two experimental parameters: 2θ displacement (d-spacing) and height of the XRD peaks. In order to optimize this refinement, the $K\alpha_2$ component was eliminated from the radiation ($K\alpha_2$ stripping) before calculations were performed.

Coherent domain (particle) size (nm) and lattice strain (%) values, which are related to the crystallinity of Ca-Mg carbonates, were jointly obtained for reciprocal directions 110, 012, 104, 110, 113 and 101, according to the Williamson-Hall method. Calculation of these values was based on both full width at half maximum (FWHM) and integral breadth (IB) diffraction profile-width criteria that, when applied independently, produced similar results. XRD peak profiles were fit toassymmetric pseudo-Voigt functions after elimination of the $K\alpha_2$ component from radiation ($K\alpha_2$stripping) and of the breadth (B) of the profiles corresponding to the instrumental profile. The lastone was performed with the Caglioty function as calculated from a very crystalline B6La standard:

$$B^2=U\cdot\tan^2\theta + V\cdot\tan\theta + W + P/\cos^2\theta$$

Where, for FWHM:

U=-0.000088255; V=0.000001221; W=-0.000088111; and P=0.000088432

And, for IB:

U=-0.000073198; V=-0.000000379; W=-0.000072512; and P=0.000074435

Size and strain (Strain nH,nK,nL=[Δd/<d>]nH,nK,nL) were determined for 110, 104, and001 hkl directions. High strain values and low size values indicate low crystallinity, which isevidenced by broader diffraction profiles [25,26]. Strain measures cell homogeneity for each direction in the carbonates studied.

## Scanning electron microscopy (SEM) study

Secondary electron (SE) images of the precipitates were 121 obtained with a field emission scanning electron microscope (FESEM) model LEO 1525, under 2-3 kV on carbon-coated samples. Selected samples were analyzed with energy dispersive X-ray analysis (EDX).

## Geochemical study

The geochemical analysis of the solutions assayed (Table 1) was performed with the geochemical computer program PHREEQC Ver.2 [27].

The activity of the dissolved species was determined and the degree of saturation evaluated. PHREEQC presents the results in terms of the saturation index (SI) for each predicted mineral. SI is defined by SI=lg (IAP/Ksp), where IAP is the ion activity product of the dissolved mineral constituents in a solubility product (Ksp) for the mineral. Thus, when SI>0 for one mineral, the solution is supersaturated in such mineral, and when SI<0, it is under saturated. Then, minerals with SI values greater than or very close to 0 could be inorganically precipitated in the media assayed [27].

The values of C, P, and $NH_4^+$ correspond to the addition of yeast extract 10 $gL^{-1}$, proteosepeptone 5 $gL^{-1}$, glucose 1 $gL^{-1}$, and calcium acetate 4 $gL^{-1}$. The total phosphorus was colorimetrically calculated in the nitrogen digests by generating the phospho molibdate complex [28]. The total carbon and nitrogen in the culture media was determined by Elemental Analysis using an elemental analyzer with a thermal conductivity detection system (THERMO SCIENTIFIC Flash 2000). C, P and $NH_4$ were the input in the program that operates under the assumption that all added organic substrates have been metabolized [28].

## Carbonic anhydrase (CA) assay

The test for CA activity was performed using the methodology described by Ramanan et al. [29]. The reaction is based on the hydration of p-nitrophenyl-acetate (p-NPA) to p-nitrophenol andacetate, which produces a yellow coloration in the presence of a CA enzyme. *H. anticariensis* was inoculated onto TSA agar (supplemented with a balanced mixture of sea salts), and incubated at 28°C for 24 hours. Subsequently, the plates were sprayed with a solution of 10 mM of p-NPA. Positive colonies changed colour and became yellow [29].

# Results

*H. anticariensis* induced bio mineralization in all of the cultures while in the control cultures were not formed precipitates. *H. anticariensis* produced spherulitic and dumbbell-shaped bioliths constituted by Ca-Mg carbonates (Figures 1, 2, 3 and 4). For 2.5% salinity, the precipitates only appeared inside the bacterial mass and were constituted by magnesian calcite containing 3 Mol %$MgCO_3$ (Table 2).

| Salinity (%) | Composition of culture media ($gL^{-1}$) | | | | | | | | | |
|---|---|---|---|---|---|---|---|---|---|---|
| | $Na^+$ | $Mg^{2+}$ | $Ca^{2+}$ | $K^+$ | $Cl^-$ | $SO_4^{2-}$ | $CO_3^{H-}$ | $Br^-$ | pH | $Mg^{2+}/Ca^{2+}$ (molar) |
| 2.5 | 7.56 | 0.89 | 1.04 | 0.26 | 15.04 | 1.91 | 0.01 | 0.04 | 7.20 | 1.40 |
| 7.5 | 22.96 | 2.71 | 1.09 | 0.78 | 41.73 | 5.80 | 0.04 | 0.13 | 7.20 | 4.10 |
| 15 | 46.01 | 5.43 | 1.16 | 1.57 | 81.68 | 1163.00 | 0.07 | 0.27 | 7.20 | 7.70 |
| 20 | 61.41 | 7.24 | 1.21 | 2.09 | 108.37 | 15.52 | 0.10 | 0.36 | 7.20 | 9.90 |

**Table 1:** Ionic composition ($gL^{-1}$) of HM with addition of sea salts (Subow. 1931) to final concentrations of 2.5%, 7.5%, 15%, and 20% (w/v). The quantities of carbon, nitrogen, and phosphorus from the decomposition of the organic nutrients in all media are the following: C=7.930 $gL^{-1}$; P=0.150 $gL^{-1}$; N=1.728 $gL^{-1}$

| Salinity (%) | Phase name | FWHM | | IB | | Unit cell parameter's (11-345) (86-2335) c | | | | | | Mg,·Ca (Formula)[d] |
|---|---|---|---|---|---|---|---|---|---|---|---|---|
| | | Size (nm) | Strain (%) | Size (nm) | Strain (%) | a = b (Å) | | c (Å) | | Volume (Å-3) | | |
| 2.5[a] | magnesian calcite | 41.610 | 0.697 | 33.580 | 0.204 | 4.958 | (0.007)[e] | 17.038 | (0.036) | 362.8 | (1.0) | 0.03, 0.97 |
| 7.5[a] | calcium dolomites | 14.090 | 0.415 | 12.819 | 0.594 | 4.874 | (0.005) | 16.354 | (0.017) | 336.9 | (0.7) | 0.36, 0.64 |
| 15[a] | calcium dolomites | 19.655 | 0.752 | 13.237 | 0.682 | 4.881 | (0.008) | 16.366 | (0.027) | 337.7 | (1.0) | 0.35, 0.65 |
| 20[a] | calcium dolomites | 18.113 | 0.729 | 15.207 | 0.869 | 4.888 | (0.010) | 16.443 | (0.036) | 340.2 | (1.4) | 0.32, 0.68 |
| | | | | | | | | | | | | |
| 2.5[b] | magnesian calcite | 50.770 | 0.790 | 43.460 | 0.285 | 4.955 | (0.006) | 17.056 | (0.032) | 362.6 | (0.9) | 0.03, 0.97 |
| 7.5[b] | calcium dolomites | 13.790 | 0.152 | 10.960 | 0. 263 | 4.893 | (0.005) | 16.448 | (0.022) | 341.1 | (0.8) | 0.31, 0.69 |
| 15 [b] | calcium dolomites | 11.960 | 0.212 | 18.790 | 0.648 | 4.875 | (0.007) | 16.361 | (0.026) | 336.7 | (1.0) | 0.35, 0.65 |
| 20 [b] | calcium dolomites | 10.880 | 0.261 | 20.140 | 0.652 | 4.883 | (0.008) | 16.363 | (0.030) | 337.9 | (1.0) | 0.35, 0.65 |

a, b: 30 d and 75 d of culture, respectively.

c: Numbers 11-345 and 86-2335 refer to JCPDS powder index files for kutnahorite and magnesian calcite used in the refinement of unit-cell parameters of calcium dolomite and magnesian calcite, respectively.

d: The Mg and Ca content are expressed in atoms per formula unit ($CO_3$•[$Mg^+Ca]_1$ ).

e: Standard deviation σ is indicated among parenthesis.

Table 2: Composition, unit-cell parametres and crystallinity of Ca-Mg carbonates precipitated by *H. anticariensis*in different culture media and incubation times.

When saline concentration was 7.5%, or higher, the precipitates formed both inside and outside of the bacterial mass though they were more abundant inside and were constituted by a different Ca-Mg carbonate containing>30 Mol % $MgCO_3$ (Table 2, Figure 1). Incubation time did not significantly affect the nature of the precipitates but, in all cases, when longer the incubation time slightly more precipitate formed.

Figure 1 shows the XRD patterns of the precipitates obtained after 30 and 75 days of culture. The variations in intensity in the reflections of the precipitates are represented in false colour. Diffraction patterns of the obtained Ca-Mg carbonate containing>30 Mol % $MgCO_3$ correspond to those of a kutnohorite-type structure [19] but this Ca-Mg carbonate phase will be hereafter named calcium dolomite (see discussion below). Table 2 shows that, in the obtained Ca-Mg carbonate precipitates, the higher $Mg^{+2}$ content the stronger lattice contraction and distortion and the smaller size of the coherent domain. In brief, calcium dolomite is characterized by a small unit-cell, coherent domain-size and high structural distortion. Table 2 presents very high values of both reflection mode widths (FWHM and IB columns), corresponding to excessively low crystallite 'Sizes (nm)' for

these Ca-dolomites with up to 0.19 Ca stoichiometric excesses per formula (last column). On the contrary, calculated values for the 'Strain (%)' are very high and show the great variability of unit-cell sizes, having these minerals in a same grain. Both low crystallite 'Size (nm)' values and high 'Strain(%)'values are only possible in very defective structures where dolomite s.str domains (whose stability structure requires strict alternation of Mg and Ca) coexist with other metastable zones with excessive Ca content.

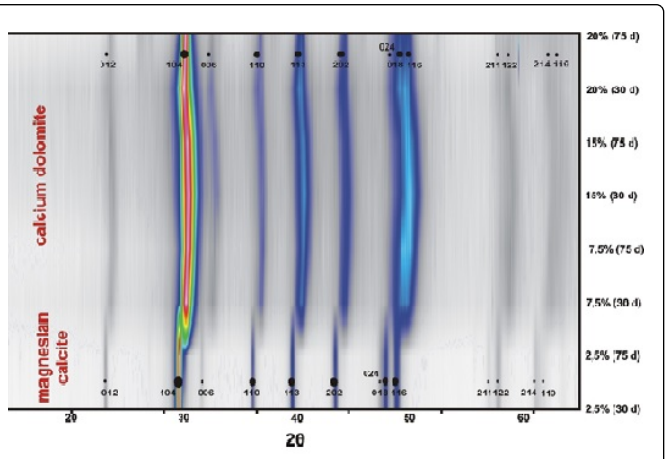


**Figure 1:** Map drawn from XRD diagrams of the culture samples at different salt concentrations and incubation times. Abscissa axis shows the 2θ for CuKα1 radiation. The different diffraction patterns are displayed along the ordinate axis. Warmer colours correspond to progressively higher intensities. Reflections of low magnesian calcite and kutnohorite are indicated in the top and the bottom of the figure, respectively.

The precipitates formed outside as well as inside the bacterial mass show similar morphologies for both magnesian calcite and calcium dolomite (Figures 3 and 4). SEM observation reveals that the spherulite morphology is dominant (Figures 2a, 2c, 3a and 4a) thought here are also dumbbell-like shapes (Figures 4b and 4c).

On the surface of the spherulites, it is common to find partially mineralized gels (Figures 2b, 3b, 3c and 4c) and mineralized bacteria with different degrees of compaction (Figures 2f, 3c and 3d). When bioliths are broken, they can have a fibrous-radiated internal structure (Figures 3e and 3f) and locally preserve also bacterial moulds (arrow in Figure 3f). Spheres and dumbbells outside of the bacterial mass have porous surfaces composed of chains of nanoparticles (crystallization units), which form complex networks (Figures 4e and 4f). Bioliths precipitated inside the mass are also made up of aggregates of nanoparticles (Figures 2d and 2h), but in such cases, they are formed on the bacterial cell envelope and associated gels (Figures 3c, 3d and 4d).

The geochemical analysis of the culture media supplemented with sea salts at concentration of 2.5%, 7.5%, 15%, and 20% and performed using PHREEQC indicates that, according to the SIvalues, the following minerals could have been inorganically precipitated from the used culture media: vaterite, dolomite, magnesite, calcite, and aragonite among carbonates, and hydroxyl apatite and struvite among the phosphates (Table 3). Nevertheless, *H. anticariensis* has only formed magnesian calcite and calcium dolomite in these media (Figure 1).

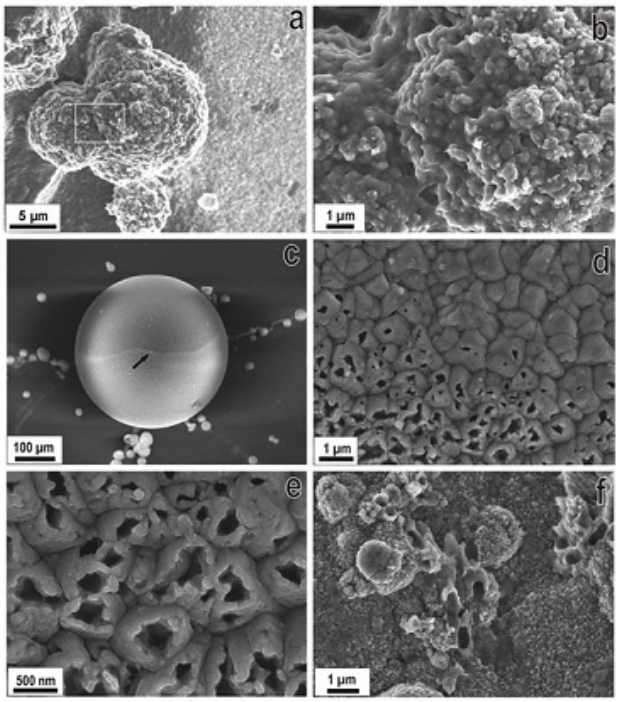


**Figure 2:** SEM images of magnesian calcite bioliths precipitated by *H, anticariensis*: (a) spherulites in formation with a large quantity of bacterial polysaccharides surrounding them; (b) close-up of the area squared in (a); (c) spherulite partially free of gels in its lower half; arrow points to the location of the inset shown in (d); (d) close-up of the surface of the spherulite shown in (b), formed by the aggregation of mineralized cells; note the occurrence of abundant nanoparticles (crystallization units) on former bacterial surfaces; (e) higher magnification view of (d); (f) mineralized bacterial cell surfaces partially included within the outer surface of one biolith.

*H. anticariensis* has only very weak CA activity since the reactive only makes it turn faintly yellow after 24 hours as well as after 5 days. This colour has been only detected within the cell mass, indicating the possibility of intracellular production of CA but only in 192 small amounts. In any case, CA is not diffused into the medium outside of the bacterial mass.

## Discussion

*H. anticariensis* in a 2.5% saline medium produces slightly magnesian calcite ($CO_3Ca_{0.930-0925}$, $Mg_{0.070-0.075}$). At higher salt concentrations (7.5%, 15% and 20%), it precipitates Mg-richcarbonate with very disordered structures whereas there is no precipitation at all in the sterile controlcultures (Table 1).

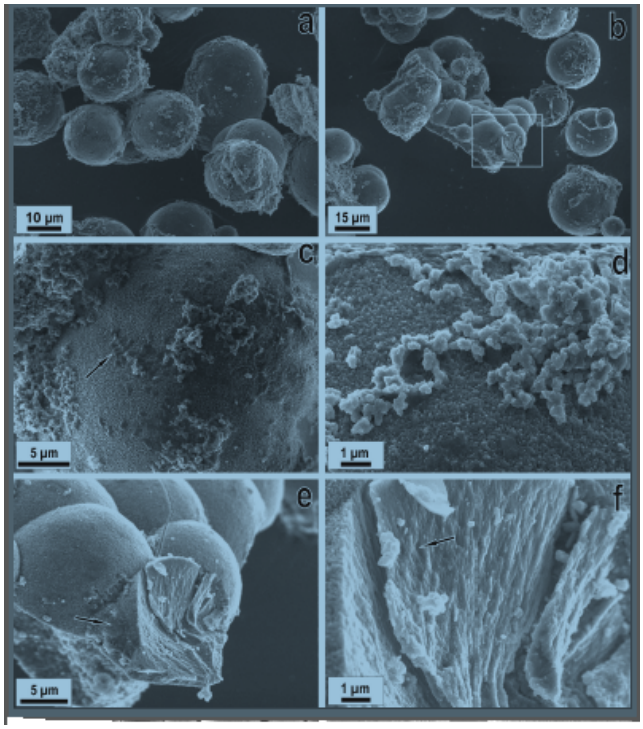


**Figure 3:** SEM images of calcium dolomite bioliths precipitated by *H. anticariensis*: (a) group of spherelitic bioliths partially attached with remnants of capsular material; (b) group of isolated spherulites, one of which forms a fibrous radiated botryoidal crust with a scratched fibrous internal structure; square area indicated the location of the inset shown in (e); (c) surface view of a biolith with abundant yet un mineralized bacterial cells on its surface (black arrow) and partially mineralized cells surrounded by carbonate nanoparticles; (d) close-up of the surface of a biolith with abundant carbonate nanoparticles surrounding moulds of degraded bacterial cells (arrows); (e) close-up of the area squared in (b) showing a group of spherulites, one of which shows its fibrous internal structure and bacterial cells above it (arrow); (f) close-up of (e), with bacterial moulds (arrow) within the fibrous crystals.

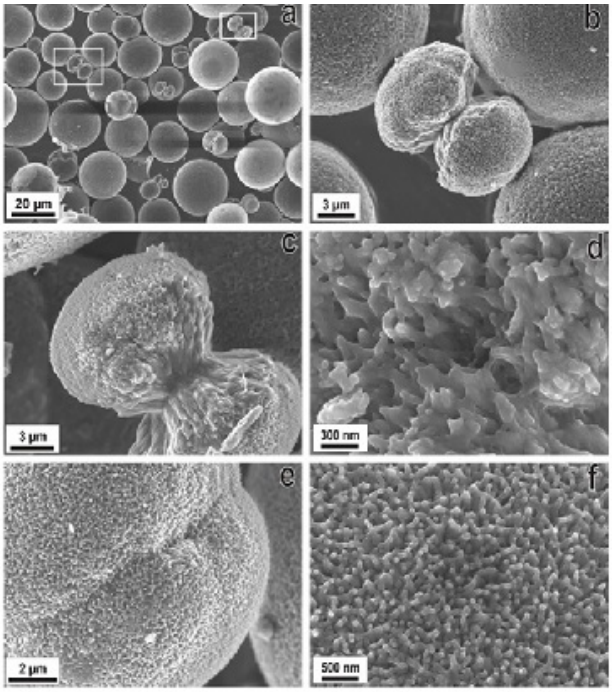


**Figure 4:**(a) SEM images of calcium dolomite (spherulites and dumbbells) precipitated by ; (b) closer view of the dumbbell in the squared area on the left of (a); (c) close up of the dumbbell shown in the squared area on the right-hand corner of (a); (d) network of carbonate nanoparticles, generally smaller than 100 nm, with abundant remnants of gelatinous material and partially mineralized bacterial moulds; (e) bioliths precipitated outside of the bacterial mass; (f)close-up of (e) showing a network of nanoparticles generally smaller than 100 nanometers with remnants of gelly-like substances and mineralized bacterial moulds.

| Mineral | Formula | Salinity (%) | | | |
|---|---|---|---|---|---|
| | | 2.5 | 7.5 | 15 | 20 |
| Aragonite | $CaCO_3$ | -1.10 | -0.58 | -0.30 | -0.08 |
| Calcite | $CaCO_3$ | -0.96 | -0.44 | -0.16 | 0.06 |
| Dolomite | $CaMg(CO_3)_2$ | -1.60 | -0.06 | 0.82 | 1.39 |
| Dolomite (disordered) | $CaMg(CO_3)_2$ | -2.15 | -0.61 | 0.27 | 0.84 |
| Huntite | $CaMg_3(CO_3)_4$ | -7.22 | -3.64 | -1.56 | -0.31 |
| Hydromagnesite | $Mg_5(CO_3)_4(OH)_2{:}4H_2O$ | -15.93 | -11.39 | -8.64 | -7.08 |
| Hydroxyapatite | $Ca_5(PO_4)_3OH$ | 10.58 | 10.00 | 9.95 | 10.11 |
| Magnesite | $MgCO_3$ | -1.22 | -0.20 | 0.40 | 0.74 |

| | | | | | |
|---|---|---|---|---|---|
| Monohydrocalcite | $CaCO_3$:$H_2O$ | -5.36 | -4.85 | -4.58 | -4.38 |
| Nesquehonite | $MgCO_3$:$3H_2O$ | -3.65 | -2.67 | -2.12 | -1.81 |
| Struvite | $MgNH_4PO_4$ | 1.64 | 2.00 | 2.36 | 2.58 |
| Vaterite | $CaCO_3$ | 15.17 | 15.69 | 15.97 | 16.19 |

Table 3: SI values for minerals in HM with addition of sea salts to final concentrations of 2.5%. 7.5%. 15%, and 20% (w/v), obtained with PHREEQC.

Strictly speaking, there is not any known mineral with the structure and chemical composition of the Mg-rich carbonate precipitated in this study. As proposed above, the term that best describes the structure and chemical composition of such carbonates is calcium-rich dolomite or calcium dolomite (i.e. $Ca^{+2}/Mg^{+2}>1$). There are not specific references for a dolomite of this type either in the IUCR PDF database or in AMCSD difdata, however kutnohorite has been used here as a database reference for calcium dolomite since both minerals have a similar structure. Kutnohorite normally shows a structural disorder in the Ca/Mn substitution, which is similar to the Ca/Mg substitution in calcium dolomite; hence this mineral was previously named Ca-Mg kutnohorite [7,19,30]. This structural disorder is caused by the excess of $Ca^{+2}$ in relation to $Mg^{+2}$ when compared to the ideal composition of dolomite (1:1 in the formula). The alternation of the $Mg^{+2}$ and $Ca^{+2}$ structural layers thus appears as somewhat uneven.

The calcium dolomite precipitated by *H. anticariensis* possess low crystallinity and high strain values, due to the disorder reflected in Ca $^{+2}/Mg^{+2}$ values different from 1 (Table 2). Neighbour sites for divalent cations in the calcium dolomite may have different size due to the variation in the local availability of $Mg^{+2}$ and $Ca^{+2}$ for the crystals being formed, thus increasing the lattice distortion. Therefore, general widening of the diffraction profiles (with very broad and frequently asymmetrical intermediate reflection positions between calcite and dolomite: Figure 1) stems not only from the small particle size but also from the high values of 216 the strain (Table 2). Calcium dolomite exhibits an extremely disordered structure, fundamentally along the c axis, in which dolomite domains (with size in the order of the crystallographic cell) alternate with calcite domains. This mineral with a disordered crystalline structure is unstable and may subsequently evolve into pure calcite and dolomite s.s. through a mechanism like spinodal decomposition [31]. This interpretation is different from that related to the proto dolomite concept [32,33]: the starting point for dolomite formation proposed here is not calcite but a disordered structure directly precipitated by bacteria and consisting of a short-range stacking of meta-stable dolomite with $Ca^{+2}/Mg^{+2}>1$ and sporadic calcite-type structures, which subsequently evolves towards more stable calcite and dolomite phases. Further evolution of these calcium dolomites involves the separation of domains with excess calcium in pure calcite and dolomite which are stable phases. So, in order to be naturally possible, it is necessary that the texture of the primitive sedimentary carbonate rock will be destroyed, while new recrystallized pure dolomite together with neo formed calcite appears as intergranular grains and/or small white veins crossing primitive carbonate rocks. This is easily observed in all geological formations with old dolomite, where higher crystallite sizes of dolomite can be measured and values of 'strain' smaller than values presented in Table 2. Also, the Mg-rich calcites also show this phenomenon, but less frequent and less significant.

Bacteria can serve as a nucleus for mineral precipitation by adsorbing cations around the cellular surface membrane, cell wall, or extracellular polymeric substance (EPS) layers [14,15,17,34,35]. The morphological study of the precipitates inside the bacterial mass shows that they were formed by the union of mineralized cells and the mineralization occurred on the cellular surface. These observations could explain the tendency of calcium-dolomite to precipitate inside the bacterial mass since most of the ions accumulated in the bacterial cell envelopes favor precipitation. Nevertheless, in the same culture, calcium-dolomite is also precipitated outside of the bacterial mass. Rivadeneyra et al. [14,35] proposes a mechanism for carbonate precipitation in which the adsorption of $Ca^{2+}$ or $Ca^{2+}$ and $Mg^{2+}$ ions, along with the release of $CO3^{2+}$ and $NH_4^+$ ions with increasing pH values may be responsible for its formation. A similar mechanism may occur in the precipitation of the calcium dolomite in our cultures. The metabolization of acetate, peptone, and yeast extract produces the $CO_3^{2+}$ and $NH_4^+$ ions needed for precipitation. Though the ions initially form inside the bacterial mass, they spread throughout the culture. As a result, they may also cause the precipitation of carbonates where there is a sufficient concentration of $Ca^{2+}$ and $Mg^{2+}$cations. This occurs despite the fact that bacterial nucleation as well as the higher $CO_3^{2+}$ and $NH_4^+$ concentration inside the bacterial mass are factors that lead to increased precipitation, as reflected in the larger quantities of precipitate in these areas. A decrease in the pH of the culture media (about 5) was observed at the beginning of the experiences, indicating a production of $CO_2$ as consequence of the degradation of carbonic organic matter: glucose and acetate. Later, pH value was increased up to 8.5-9, showing a degradation of the nitrogenous organic matter: yeast extract and peptone.

This research study has also analysed the enzymatic carbonic anhydrase activity of *H.anticariensis* to better understand its possible relation to carbonate precipitation. The CA enzyme catalyses the reversible hydration of $CO_2$ to bicarbonate and is involved in biological carbonate precipitation by various types of marine organisms [36,37]. It could also be responsible for the sequestration of a significant fraction of $CO_2$ by heterotrophic bacteria in natural underground environments [38]. Nevertheless, its role in carbonate precipitation by bacteria is still unclear. *Hanticariensis* produces a very weak staining, caused by the production of a small amount of enzyme, and only in the cell mass. However, in the conditions studied, it has been found to present a high capacity for carbonate precipitation. In addition, the carbonates have also been formed outside the bacterial mass, where there was no enzyme since it had not diffused into the medium. This seems toindicate the enzyme is not absolutely necessary for the precipitation of carbonates by *H. anticariensis.* When the mineral saturation index (SI) was calculated with the geochemical PHREEQC computer program (Table 3), all of the organic material was assumed to be metabolized. According to this SI, different carbonates and phosphates can be inorganically precipitated. However, *H. anticariensis*

only formed magnesium calcite and calcium dolomite, whereas there was no precipitation at all in the sterile control cultures. This seems to indicate that the progressive liberation of $CO_3^{2+}$ and $NH_4^+$induces precipitation more effectively than high levels of these ions. The precipitation of both minerals can be regarded as biologically-induced precipitation [39] since their formation is related to bacteria growth. In this type of biomineralization, the bacteria have both an active and passive role in the precipitation process. The fact that calcium dolomite was formed inside as well as outside of the bacterial mass shows that in *H. anticariensis* cultures, both types of precipitation occur.

Spheroidal and dumbbell morphologies of the magnesian calcite and calcium dolomite bioliths precipitated by *H. anticariensis*are common to other biogenic carbonates [15,17,19]. The behaviour and morphologies of bacterial precipitates are influenced by the viscosity of medium [40]. In fact, in a gellified culture medium with calcium and magnesium (such as the one in this study), the diffusion pattern of the cations and metabolites in the culture medium produces spatial-temporal concentration gradients that create super saturation conditions. These conditions influence the morphology of the precipitates, as observed in previous research [19,41]. In both cases, spherulites and dumbbells are composed of aggregates and/or chains of nanoparticles (or Nano globules [42]) that actually are crystallization units. It has recently been reported that the nucleation of Ca-carbonate occurs on such nanoparticles in relation to an amorphous Ca-phosphate precursor [35]. Furthermore, it has been proposed that the occurrence of nanoglobules can be regarded as biosignatures which are preserved in rock layers [43]. Nanometre-sized spheres with granulated texture have also been observed in natural dolomite at different locations dating back to various geologic ages, from Recent to Archean [43]. This research has also found nanoglobule chains in the spherulites outside the bacterial mass. The contribution of bacterial activity to carbonate precipitation on Earth's surface is widely acknowledged. However, the precipitation of dolomite is still controversial. In fact, many researchers refer to this as the dolomite problem [21]. Dolomite is a mineral that is abundantly found in natural environments since it was formed in massive quantities in ancient geological periods. However, this state of affairs changed dramatically in subsequent eras, and now dolomite is barely precipitated. These dolomite formations are thus still something of a mystery, and if their origin and formation mechanism were known, this would significantly contribute to the knowledge of past and current biogeochemical processes [11,21,22]. It has been demonstrated that aerobic bacteria isolated from soils and the water–sediment interface [4,6,44-46] favour dolomite precipitation. In addition, sulfate-reducing bacteria have been related to dolomite production under anoxic conditions [16,22,46]. This signifies that microbial processes may have been involved in dolomite formation in natural environments. Our results suggest that, in certain natural habitats, calcium-rich dolomite produced by biological activity could be a precursor phase for dolomite. It is also our assertion that the study of other calcium dolomite produced by bacterial mediation can also lead to a better understanding of dolomite formation as well as that of carbonate precipitation processes.

## Conclusions

This research shows that *H. anticariensis* has the biomineralization capability to precipitate magnesian calcite and calcium dolomite. Calcium dolomite has very small particle size and high lattice distortion because of Mg and $Ca^{+2}$ randomly occupy cation sites in the structure of their hombohedral carbonate. The excess of $Ca^{+2}$ in relation to $Mg^{+2}$ precludes formation of pure dolomite where $Mg^{+2}$ and $Ca^{+2}$ occur in a 1:1 stoichiometry. We suggest that calcium-rich dolomite produced by biological activity is a precursory phase of dolomite through its transformation into calcite and dolomite, which occurs after a long period of time. It would explain why no dolomite s.s.is absent in recent sediments. In contrast, such deposits contain low crystallinity non-stoichiometric disordered Mg-rich carbonates similar to the calcium dolomite precipitated by *H. anticariensis*. Accordingly, the bacterial precipitation of calcium dolomite at different seawater salinities provides a new dimension to the dolomite problem and supports the hypothesis of its bacterially mediated massive precipitation in certain periods of the geological time. The scarcity of calcium dolomite in Nature could be more closely related to its subsequent transformation into other more stable minerals rather than to its lack of precipitation in these environments.

## Acknowledgements

This research was carried out as part of the FP7 project, $CO_2$ Sol Stock-Bio based geological $CO_2$ storage, funded by the European Union ($7^{th}$ Framework Programme). Financial Support from the projects CGL2012-32169 (MCI), P11-RNM-7067, RNM-208 and RNM-3715 (JA) is also acknowledged.

## References

1. Ehrlich HL, Newman DK (2008) Geomicrobiology. ($5^{th}$edtn), CRC press.
2. McKay DS, Gibson EK Jr, Thomas Keprta KL, Vali H, Romanek CS, et al. (1996) Search for past life on Mars: possible relic biogenic activity in martian meteorite ALH84001. Science 273: 924-930.
3. Allen CC, Albert FG, Chafetz HS, Combie J, Graham CR, et al. (2000) Microscopic physical biomarkers in carbonate hot springs: implications in the search for life on Mars. Icarus 147: 49-67.
4. Rivadeneyra M, Ramos Cormenzana A, Garcia Cervigon A (1985) Etude de l'influencedurapport Mg/Casur la formation de carbonate par des bactériestelluriques. Canadian J Microbiol 31: 229-231.
5. Rivadeneyra MA, Delgado G, Soriano M, Ramos Cormenzana A, Delgado R (1999) Biomineralization of carbonates by Marinococcusalbus and Marinococcushalophilus isolated from the Salar de Atacama (Chile). Curr Microbiol 39: 53-57.
6. Rivadeneyra MA, Delgado G, Soriano M, Ramos Cormenzana A, Delgado R (2000) Precipitation of carbonates by Nesterenkoniahalobia in liquid media. Chemosphere 41: 617-624.
7. Rivadeneyra MA, Martin Algarra A, Sánchez Navas A, Martíin Ramos D (2006) Carbonate and phosphate precipitation by Chromohalobactermarismortui. Geomicrobiol J 23: 89-101.
8. Castanier S, Le MétayerLevrel G, Perthuisot JP (1999) Ca-carbonates precipitation and limestone genesis- the microbiogeologist point of view. Sediment Geol 126: 9-23.
9. Knorre HV, Krumbein WE (2000) Bacterial calcification, in Microbial sediments, Springer.
10. Riding R (2000) Microbial carbonates: the geological record of calcified bacterial–algal mats and biofilms. Sedimentol 47: 179-214.
11. Wright DT, Wacey D (2005) Precipitation of dolomite using sulphate-reducing bacteria from the Coorong Region, South

Australia: significance and implications. Sedimentol 52: 987-1008.

12. Delgado G, Delgado R, Parraga J, Rivadeneyra MA, Aranda V (2008) Precipitation of carbonates and phosphates by bacteria in extract Solutions from a semi-arid saline soil. Influence of $Ca^{2+}$ and $Mg^{2+}$ concentrations 360 and Mg2+/Ca2+ molar ratio in Biomineralization. Geomicrobiol J 25: 1-13.
13. Morita RY (1980) Calcite precipitation by marine bacteria. Geomicrobiol J 2: 63-82.
14. Rivadeneyra MA, Ramos Cormenzana A, Delgado G, Delgado R (1996) Process of Carbonate Precipitation by Deleyahalophila. Curr Microbiol 32: 308-313.
15. Braissant O, Cailleau G, Dupraz C, Verrecchia EP (2003) Bacterially induced mineralization of calcium carbonate in terrestrial environments: the role of exopolysaccharides and amino acids. J Sediment Res 73: 485- 490.
16. Van Lith Y, Warthmann R, Vasconcelos C, McKenzie JA (2003) Microbial fossilization in carbonate sediments: a result of the bacterial surface involvement in dolomite precipitation. Sedimentol 50: 237-245.
17. Rivadeneyra MA, Delgado R, Parraga J, Ramos Cormenzana A, Delgado G (2006) Precipitation of minerals by 22 species of moderately halophilic bacteria in artificial marine salts media: influence of salt concentration. Folia microbial 51: 445-453.
18. Sánchez Roman M, Rivadeneyra MA, Vasconcelos C, McKenzie JA (2007) Biomineralization of carbonate and phosphate by moderately halophilic bacteria. FEMS Microbiol Ecol 61: 273-284.
19. Sanchez Navas A, MartinAlgarra A, Rivadeneyra MA, Melchor S, Martin Ramos JD (2009) Crystal-Growth Behavior in Ca- Mg Carbonate Bacterial Spherulites. Cryst Growth Des 9: 2690-2699.
20. Peacor DR, Essene EJ, Gaines A (1987) Petrologic and crystal-384 chemical implications of cation order-disorder in kutnahorite [CaMn $(CO_3)_2$. Am Mineral 72: 319-328.
21. Burns SJ, Mckenzie JA, Vasconcelos C (2000) Dolomite formation and bio geochemical cycles in the Phanerozoic. Sedimentol 47: 49-61.
22. Vasconcelos C, McKenzie JA, Bernasconi S, Grujic D, Tiens AJ (1995) Microbial mediation as a possible mechanism for natural dolomite formation at low temperatures. Nat 377: 220-222.
23. Martínez Canovas MJ, Quesada E, Martinez Checa F, Bejar V (2004) A taxonomic study to establish the relationship between exopolysaccharide-producing bacterial strains living in diverse hypersaline habitats. Curr Microbiol 48: 348-353.
24. Martínez Canovas MJ, Bejar V, Martínez Checa F, Quesada E (2004) Halomonasanticariensis sp. nov., from Fuente de Piedra, a saline-wetland wildfowl reserve in Málaga, southern Spain. Int J Syst Evol Microbiol 54: 1329-1332.
25. Martin J (2004) Using X Powder: A software package for Powder X-Ray diffraction analysis. DLGR 1001: 105.
26. Martín Ramos J, Cambeses A, Lopez Galindo A, Scarrow J, Diaz Hernandez J (2012) Pathways for quantitative analysis by X-Ray diffraction: In Tech Open Access Publisher.
27. Parkhurst DL, Appelo C (1999) User's guide to PHREEQC (Version 2): A computer program for speciation, batch-reaction, one-dimensional transport, and inverse geochemical calculations.
28. Page AL (1982) Methods of soil analysis. Part 2 ($2^{nd}$edtn), Chemical and microbiological properties: American Society of Agronomy, Soil Science Society of America.
29. Ramanan R, Kannan K, Sivanesan SD, Mudliar S, Tripathi AK, et al. (2009) Bio sequestration of carbon dioxide using carbonic anhydrase enzyme purified from Citrobacterfreundii. World J MicrobiolBiotechnol 25: 981-987.
30. González Muñoz MT, De Linares C, Martínez Ruiz F, Morcillo F, Martín-Ramos D, et al. (2008) Ca-Mg kutnahorite and struvite production by Idiomarina strains at modern seawater salinities. Chemosphere 72: 465-472.
31. Clarke J, Hastie J, Kihlborg L, Metselaar R, Thackeray M (1994) Definitions of terms relating to phase transitions of the solid state (iupac recommendations 1994). Pure Appl Chem 66: 577-594.
32. Gaines AM (1977) Protodolomite redefined. J Sediment Res 47.
33. Ohde S, Kitano Y (1981) Protodolomite in Daito-jima, Okinawa. Geochem J 15: 199-207.
34. Rivadeneyra MA, Delgado G, Ramos-Cormenzana A, Delgado R (1998) Biomineralization of carbonates by Halomonaseurihalina in solid and liquid media with different salinities: crystal formation sequence. Res Microbiol 149: 277-287.
35. Rivadeneyra MA, Martin Algarra A, Sanchez-Roman M, Sanchez Navas A, Martin Ramos JV (2010) Amorphous Ca-phosphate precursors for Ca-carbonate biominerals mediated by Chromo halobactermarismortui. ISME J 4: 922-932.
36. Bond GM, Stringer J, Brandvold DK, Simsek FA, Medina MG, et al. (2001) Development of integrated system for biomimetic CO2 sequestration using the enzyme carbonic anhydrase. Energy & Fuels 15: 309-316.
37. Bond GM, Liu N, Abel A, McPherson MJ, Stringer J (2004) Biomimetic Sequestration of $CO_2$ in Carbonate Form: Role of Produced Waters and Other Brines. Prepr Pap Am ChemSocDiv Fuel Chem 49: 420.
38. Sanchez Moral S, Canaveras J, Laiz L, Bedoya J, Luque L (2003) Biomediated precipitation of calcium carbonate metastable phases in hypogean environments: a short review. Geomicrobiol J 20: 491-500.
39. Lowenstam HA, Weiner S (1989) On biomineralization: Oxford University Press.
40. Buczynski C, Chafetz HS (1991) Habit of bacterially induced precipitates of calcium carbonate and the influence of medium vicosity on mineralogy. J Sediment Res 61: 226-233.
41. Gonzalez Munoz MT, Chekroun KB, Aboud AB, Arias JB, Rodriguez Gallego M (2000) Bacterially induced Mg-calcite formation: role of $Mg^{2+}$ in development of crystal morphology. J Sediment Res 70: 559-564.
42. Aloisi G, Gloter A, Kruger M, Wallmann K, Guyot F, et al. (2006) Nucleation of calcium carbonate on bacterial nanoglobules. Geol 34: 1017-1020.
43. Sanchez Roman M, Vasconcelos C, Schmid T, Dittrich M, McKenzie JA, et al. (2008) Aerobic microbial dolomite at the nanometer scale: Implications for the geologic record. Geol 36: 879-882.
44. Rivadeneyra MA, Delgado R, Delgado G, Moral AD, Ferrer M, et al. (1993) Precipitation of carbonates by Bacillus sp. isolated from saline soils. Geomicrobiol J 11: 175-184.
45. Sanchez Roman M, Vasconcelos C, Warthmann R, Rivadeneyra M, McKenzie JA (2009) Microbial Dolomite Precipitation under

Aerobic Conditions: Results from Brejo do Espinho Lagoon (Brazil) and Culture Experiments: IAS Spec Publ 41: 167-178.

46. Sanchez Roman M, McKenzie JA, Wagener ADLR, Rivadeneyra MA, Vasconcelos C (2009) Presence of sulfate does not inhibit low-temperature dolomite precipitation. Earth Planet Sci Lett 285: 131-139.